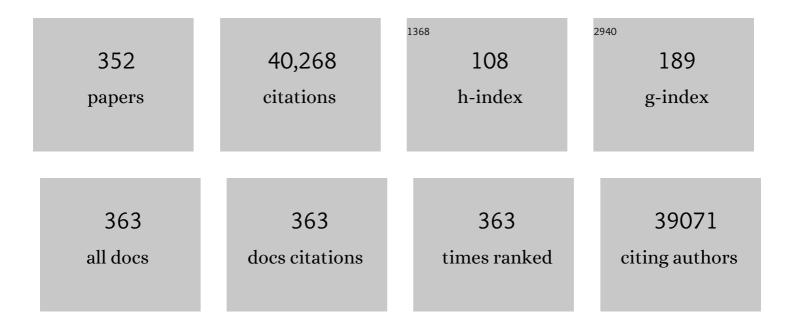
List of Publications by Year in descending order

Source: https://exaly.com/author-pdf/6982584/publications.pdf

Version: 2024-02-01



#	Article	IF	CITATIONS
1	Merging DNA Probes with Nanotechnology for RNA Imaging In vivo. Current Analytical Chemistry, 2022, 18, 622-629.	0.6	2
2	Tailoring Aggregation Extent of Photosensitizers to Boost Phototherapy Potency for Eliciting Systemic Antitumor Immunity. Advanced Materials, 2022, 34, e2106390.	11.1	65
3	Toxicity of manufactured nanomaterials. Particuology, 2022, 69, 31-48.	2.0	63
4	Combinational application of metal–organic frameworksâ€based nanozyme and nucleic acid delivery in cancer therapy. Wiley Interdisciplinary Reviews: Nanomedicine and Nanobiotechnology, 2022, 14, e1773.	3.3	16
5	A Photosensitizer Discretely Loaded Nanoaggregate with Robust Photodynamic Effect for Local Treatment Triggers Systemic Antitumor Responses. ACS Nano, 2022, 16, 3070-3080.	7.3	38
6	Selenopeptide Nanomedicine Activates Natural Killer Cells for Enhanced Tumor Chemoimmunotherapy. Advanced Materials, 2022, 34, e2108167.	11.1	32
7	Radiolabeled peptide probe for tumor imaging. Chinese Chemical Letters, 2022, 33, 3361-3370.	4.8	7
8	Multivalent Engineering of Exosomes with Activatable Aptamer Probes for Specific Regulation and Monitoring of Cell Targeting. Analytical Chemistry, 2022, 94, 3840-3848.	3.2	11
9	Ultrafast Growth of Highly Conductive Graphene Films by a Single Subsecond Pulse of Microwave. ACS Nano, 2022, 16, 6676-6686.	7.3	3
10	Precision design of engineered nanomaterials to guide immune systems for disease treatment. Matter, 2022, 5, 1162-1191.	5.0	11
11	Oncolytic peptide nanomachine circumvents chemo resistance of renal cell carcinoma. Biomaterials, 2022, 284, 121488.	5.7	5
12	Spatially Selective Monitoring of Subcellular Enzyme Dynamics in Response to Mitochondriaâ€Targeted Photodynamic Therapy. Angewandte Chemie - International Edition, 2022, 61, .	7.2	19
13	Air pollution: A culprit of lung cancer. Journal of Hazardous Materials, 2022, 434, 128937.	6.5	51
14	Reducing Postoperative Recurrence of Early‣tage Hepatocellular Carcinoma by a Woundâ€Targeted Nanodrug. Advanced Science, 2022, 9, e2200477.	5.6	15
15	Innenrücktitelbild: Spatially Selective Monitoring of Subcellular Enzyme Dynamics in Response to Mitochondriaâ€Targeted Photodynamic Therapy (Angew. Chem. 28/2022). Angewandte Chemie, 2022, 134, .	1.6	0
16	Mild Acidosisâ€Directed Signal Amplification in Tumor Microenvironment via Spatioselective Recruitment of DNA Amplifiers. Angewandte Chemie - International Edition, 2022, 61, .	7.2	13
17	Upconversion Luminescenceâ€Boosted Escape of DNAzyme from Endosomes for Enhanced Geneâ€Silencing Efficacy. Angewandte Chemie - International Edition, 2022, 61, .	7.2	15
18	Upconversion Luminescenceâ€Boosted Escape of DNAzyme from Endosomes for Enhanced Geneâ€Silencing Efficacy. Angewandte Chemie. 2022. 134	1.6	2

#	Article	IF	CITATIONS
19	Research trends in biomedical applications of two-dimensional nanomaterials over the last decade – A bibliometric analysis. Advanced Drug Delivery Reviews, 2022, 188, 114420.	6.6	25
20	Fractionated regimen-suitable immunoradiotherapy sensitizer based on ultrasmall Fe4Se2W18 nanoclusters enable tumor-specific radiosensitization augment and antitumor immunity boost. Nano Today, 2021, 36, 101003.	6.2	26
21	Nanomedicine enables spatiotemporally regulating macrophage-based cancer immunotherapy. Biomaterials, 2021, 268, 120552.	5.7	23
22	New Insights from Chemical Biology: Molecular Basis of Transmission, Diagnosis, and Therapy of SARS-CoV-2. CCS Chemistry, 2021, 3, 1501-1528.	4.6	12
23	Molybdenum derived from nanomaterials incorporates into molybdenum enzymes and affects their activities in vivo. Nature Nanotechnology, 2021, 16, 708-716.	15.6	153
24	Organelle‧pecific Photoactivation of DNA Nanosensors for Precise Profiling of Subcellular Enzymatic Activity. Angewandte Chemie, 2021, 133, 9005-9013.	1.6	20
25	Organelleâ€5pecific Photoactivation of DNA Nanosensors for Precise Profiling of Subcellular Enzymatic Activity. Angewandte Chemie - International Edition, 2021, 60, 8923-8931.	7.2	97
26	Controllable Selfâ€Assembly of Peptideâ€Cyanine Conjugates In Vivo as Fineâ€Tunable Theranostics. Angewandte Chemie - International Edition, 2021, 60, 7809-7819.	7.2	51
27	Controllable Selfâ€Assembly of Peptideâ€Cyanine Conjugates In Vivo as Fineâ€Tunable Theranostics. Angewandte Chemie, 2021, 133, 7888-7898.	1.6	10
28	Development of a Cancer Vaccine Using In Vivo Clickâ€Chemistryâ€Mediated Active Lymph Node Accumulation for Improved Immunotherapy. Advanced Materials, 2021, 33, e2006007.	11.1	70
29	One-Step Synthesis of Single-Stranded DNA-Bridged Iron Oxide Supraparticles as MRI Contrast Agents. Nano Letters, 2021, 21, 2793-2799.	4.5	19
30	X-ray-Based Techniques to Study the Nano–Bio Interface. ACS Nano, 2021, 15, 3754-3807.	7.3	60
31	A bibliometric analysis: Research progress and prospects on transition metal dichalcogenides in the biomedical field. Chinese Chemical Letters, 2021, 32, 3762-3770.	4.8	17
32	Tumor-discriminating Nanoceria Antioxidant Enables Protection Against Acute Kidney Injury Without Compromising Chemotherapeutic Effects. Chemical Research in Chinese Universities, 2021, 37, 621-622.	1.3	1
33	Selfâ€Assembly of Copper–DNAzyme Nanohybrids for Dual atalytic Tumor Therapy. Angewandte Chemie, 2021, 133, 14445-14449.	1.6	16
34	Selfâ€Assembly of Copper–DNAzyme Nanohybrids for Dual atalytic Tumor Therapy. Angewandte Chemie - International Edition, 2021, 60, 14324-14328.	7.2	100
35	Second near-infrared window persistent luminescence nanomaterials for in vivo bioimaging. Science China Chemistry, 2021, 64, 1439-1440.	4.2	1
36	Highly Stable Silica-Coated Bismuth Nanoparticles Deliver Tumor Microenvironment-Responsive Prodrugs to Enhance Tumor-Specific Photoradiotherapy. Journal of the American Chemical Society, 2021, 143, 11449-11461.	6.6	51

#	Article	IF	CITATIONS
37	Bacterial cytoplasmic membranes synergistically enhance the antitumor activity of autologous cancer vaccines. Science Translational Medicine, 2021, 13, .	5.8	109
38	The Underlying Function and Structural Organization of the Intracellular Protein Corona on Graphdiyne Oxide Nanosheet for Local Immunomodulation. Nano Letters, 2021, 21, 6005-6013.	4.5	63
39	Nanotoxicology and nanomedicine: The Yin and Yang of nano-bio interactions for the new decade. Nano Today, 2021, 39, 101184.	6.2	67
40	Ultrafast Growth of Large Area Graphene on Si Wafer by a Single Pulse Current. Molecules, 2021, 26, 4940.	1.7	4
41	X-ray-facilitated redox cycling of nanozyme possessing peroxidase-mimicking activity for reactive oxygen species-enhanced cancer therapy. Biomaterials, 2021, 276, 121023.	5.7	34
42	Plasmonic AuPt@CuS Heterostructure with Enhanced Synergistic Efficacy for Radiophotothermal Therapy. Journal of the American Chemical Society, 2021, 143, 16113-16127.	6.6	85
43	Rational Design of Nanomaterials for Various Radiationâ€Induced Diseases Prevention and Treatment. Advanced Healthcare Materials, 2021, 10, e2001615.	3.9	26
44	Reactive Oxygen Speciesâ€Regulating Strategies Based on Nanomaterials for Disease Treatment. Advanced Science, 2021, 8, 2002797.	5.6	149
45	3D Imaging and Quantification of the Integrin at a Single-Cell Base on a Multisignal Nanoprobe and Synchrotron Radiation Soft X-ray Tomography Microscopy. Analytical Chemistry, 2021, 93, 1237-1241.	3.2	20
46	Accelerated discovery of superoxide-dismutase nanozymes via high-throughput computational screening. Nature Communications, 2021, 12, 6866.	5.8	62
47	Time-Resolved Activation of pH Sensing and Imaging in Vivo by a Remotely Controllable DNA Nanomachine. Nano Letters, 2020, 20, 874-880.	4.5	56
48	Nd <sup>3+</sup> ‣ensitized Upconversion Metal–Organic Frameworks for Mitochondriaâ€Targeted Amplified Photodynamic Therapy. Angewandte Chemie, 2020, 132, 2656-2660.	1.6	10
49	Two-dimensional nanomaterials beyond graphene for antibacterial applications: current progress and future perspectives. Theranostics, 2020, 10, 757-781.	4.6	152
50	Single-Particle Analysis for Structure and Iron Chemistry of Atmospheric Particulate Matter. Analytical Chemistry, 2020, 92, 975-982.	3.2	24
51	Nd <sup>3+</sup> â€Sensitized Upconversion Metal–Organic Frameworks for Mitochondriaâ€Targeted Amplified Photodynamic Therapy. Angewandte Chemie - International Edition, 2020, 59, 2634-2638.	7.2	175
52	Stimuli-Responsive Small-on-Large Nanoradiosensitizer for Enhanced Tumor Penetration and Radiotherapy Sensitization. ACS Nano, 2020, 14, 10001-10017.	7.3	93
53	Implications of the Human Gut–Brain and Gut–Cancer Axes for Future Nanomedicine. ACS Nano, 2020, 14, 14391-14416.	7.3	30
54	Progress, challenges, and future of nanomedicine. Nano Today, 2020, 35, 101008.	6.2	135

#	Article	IF	CITATIONS
55	Density Functional Theory-Based Method to Predict the Activities of Nanomaterials as Peroxidase Mimics. ACS Catalysis, 2020, 10, 12657-12665.	5.5	92
56	Suppressing the Radiation-Induced Corrosion of Bismuth Nanoparticles for Enhanced Synergistic Cancer Radiophototherapy. ACS Nano, 2020, 14, 13016-13029.	7.3	42
57	Nano-bio interactions: the implication of size-dependent biological effects of nanomaterials. Science China Life Sciences, 2020, 63, 1168-1182.	2.3	58
58	Combination of tumour-infarction therapy and chemotherapy via the co-delivery of doxorubicin and thrombin encapsulated in tumour-targeted nanoparticles. Nature Biomedical Engineering, 2020, 4, 732-742.	11.6	99
59	An orthogonally regulatable DNA nanodevice for spatiotemporally controlled biorecognition and tumor treatment. Science Advances, 2020, 6, eaba9381.	4.7	105
60	A smart DNA nanodevice for ATP-activatable bioimaging and photodynamic therapy. Science China Chemistry, 2020, 63, 1490-1497.	4.2	18
61	Clinically Approved Carbon Nanoparticles with Oral Administration for Intestinal Radioprotection via Protecting the Small Intestinal Crypt Stem Cells and Maintaining the Balance of Intestinal Flora. Small, 2020, 16, e1906915.	5.2	51
62	Graphdiyne nanoradioprotector with efficient free radical scavenging ability for mitigating radiation-induced gastrointestinal tract damage. Biomaterials, 2020, 244, 119940.	5.7	58
63	Ultrasmall BiOI Quantum Dots with Efficient Renal Clearance for Enhanced Radiotherapy of Cancer. Advanced Science, 2020, 7, 1902561.	5.6	63
64	BiO <sub>2–<i>x</i></sub> Nanosheets as Radiosensitizers with Catalase-Like Activity for Hypoxia Alleviation and Enhancement of the Radiotherapy of Tumors. Inorganic Chemistry, 2020, 59, 3482-3493.	1.9	64
65	Immunological Responses Induced by Blood Protein Coronas on Two-Dimensional MoS <sub>2</sub> Nanosheets. ACS Nano, 2020, 14, 5529-5542.	7.3	82
66	A Heterojunction Structured WO <sub>2.9</sub> -WSe <sub>2</sub> Nanoradiosensitizer Increases Local Tumor Ablation and Checkpoint Blockade Immunotherapy upon Low Radiation Dose. ACS Nano, 2020, 14, 5400-5416.	7.3	104
67	Glucose-responsive cascaded nanocatalytic reactor with self-modulation of the tumor microenvironment for enhanced chemo-catalytic therapy. Materials Horizons, 2020, 7, 1834-1844.	6.4	56
68	Grapheneâ€Based Smart Platforms for Combined Cancer Therapy. Advanced Materials, 2019, 31, e1800662.	11.1	233
69	Nearâ€Infrared Lightâ€Initiated Hybridization Chain Reaction for Spatially and Temporally Resolved Signal Amplification. Angewandte Chemie, 2019, 131, 15019-15023.	1.6	101
70	Nearâ€Infrared Lightâ€Initiated Hybridization Chain Reaction for Spatially and Temporally Resolved Signal Amplification. Angewandte Chemie - International Edition, 2019, 58, 14877-14881.	7.2	148
71	A Dualâ€Response DNA Probe for Simultaneously Monitoring Enzymatic Activity and Environmental pH Using a Nanopore. Angewandte Chemie - International Edition, 2019, 58, 14929-14934.	7.2	50
72	The pharmaceutical multi-activity of metallofullerenol invigorates cancer therapy. Nanoscale, 2019, 11, 14528-14539.	2.8	16

#	Article	IF	CITATIONS
73	Stability of Ligands on Nanoparticles Regulating the Integrity of Biological Membranes at the Nano–Lipid Interface. ACS Nano, 2019, 13, 8680-8693.	7.3	59
74	Cellular Responses to Exposure to Outdoor Air from the Chinese Spring Festival at the Air–Liquid Interface. Environmental Science & Technology, 2019, 53, 9128-9138.	4.6	9
75	Graphdiyne: The Fundamentals and Application of an Emerging Carbon Material. Advanced Materials, 2019, 31, e1904885.	11.1	33
76	Emerging Delivery Strategies of Carbon Monoxide for Therapeutic Applications: from CO Gas to CO Releasing Nanomaterials. Small, 2019, 15, e1904382.	5.2	79
77	Clinical Nanomaterials: A Safeâ€byâ€Đesign Strategy towards Safer Nanomaterials in Nanomedicines (Adv.) Tj E	TQq1_1 0.7	784314 rgBT
78	Nano as a Rosetta Stone: The Global Roles and Opportunities for Nanoscience and Nanotechnology. ACS Nano, 2019, 13, 10853-10855.	7.3	16
79	A Dualâ€Response DNA Probe for Simultaneously Monitoring Enzymatic Activity and Environmental pH Using a Nanopore. Angewandte Chemie, 2019, 131, 15071-15076.	1.6	8
80	Engineered Graphene Oxide Nanocomposite Capable of Preventing the Evolution of Antimicrobial Resistance. ACS Nano, 2019, 13, 11488-11499.	7.3	84
81	<i>Bacillus subtilis</i> causes dissolution of ceria nanoparticles at the nano–bio interface. Environmental Science: Nano, 2019, 6, 216-223.	2.2	15
82	Exploring the Interaction of Fullerenol with Key Digestive Proteases Using Raman-Based Frequency-Shift Sensing and Molecular Simulation Analysis. ACS Applied Bio Materials, 2019, 2, 2946-2954.	2.3	2
83	Precision Nanomedicine Development Based on Specific Opsonization of Human Cancer Patient-Personalized Protein Coronas. Nano Letters, 2019, 19, 4692-4701.	4.5	87
84	An Acidicâ€Microenvironmentâ€Driven DNA Nanomachine Enables Specific ATP Imaging in the Extracellular Milieu of Tumor. Advanced Materials, 2019, 31, e1901885.	11.1	97
85	Simultaneous enzyme mimicking and chemical reduction mechanisms for nanoceria as a bio-antioxidant: a catalytic model bridging computations and experiments for nanozymes. Nanoscale, 2019, 11, 13289-13299.	2.8	100
86	Strategies based on metal-based nanoparticles for hypoxic-tumor radiotherapy. Chemical Science, 2019, 10, 6932-6943.	3.7	111
87	Ultrasensitive Detection of Circulating Tumor DNA of Lung Cancer via an Enzymatically Amplified SERS-Based Frequency Shift Assay. ACS Applied Materials & Interfaces, 2019, 11, 18145-18152.	4.0	65
88	Influence of Surface Charge on the Phytotoxicity, Transformation, and Translocation of CeO <sub>2</sub> Nanoparticles in Cucumber Plants. ACS Applied Materials & Interfaces, 2019, 11, 16905-16913.	4.0	45
89	An Extendable Star-Like Nanoplatform for Functional and Anatomical Imaging-Guided Photothermal Oncotherapy. ACS Nano, 2019, 13, 4379-4391.	7.3	65
90	Elemental analysis and imaging of sunscreen fingermarks by X-ray fluorescence. Analytical and Bioanalytical Chemistry, 2019, 411, 4151-4157.	1.9	7

#	Article	IF	CITATIONS
91	Screen efficiency comparisons of decision tree and neural network algorithms in machine learning assisted drug design. Science China Chemistry, 2019, 62, 506-514.	4.2	10
92	Comparative study of core- and surface-radiolabeling strategies for the assembly of iron oxide nanoparticle-based theranostic nanocomposites. Nanoscale, 2019, 11, 5909-5913.	2.8	5
93	Surface-Functionalized Modified Copper Sulfide Nanoparticles Enhance Checkpoint Blockade Tumor Immunotherapy by Photothermal Therapy and Antigen Capturing. ACS Applied Materials & Interfaces, 2019, 11, 13964-13972.	4.0	105
94	Recent advances of stimuli-responsive systems based on transition metal dichalcogenides for smart cancer therapy. Journal of Materials Chemistry B, 2019, 7, 2588-2607.	2.9	29
95	Enhanced Generation of Non-Oxygen Dependent Free Radicals by Schottky-type Heterostructures of Au–Bi <sub>2</sub> S <sub>3</sub> Nanoparticles <i>via</i> X-ray-Induced Catalytic Reaction for Radiosensitization. ACS Nano, 2019, 13, 5947-5958.	7.3	126
96	A Safeâ€byâ€Design Strategy towards Safer Nanomaterials in Nanomedicines. Advanced Materials, 2019, 31, e1805391.	11.1	109
97	Progress and Prospects of Graphdiyneâ€Based Materials in Biomedical Applications. Advanced Materials, 2019, 31, e1804386.	11.1	124
98	Precise design of nanomedicines: perspectives for cancer treatment. National Science Review, 2019, 6, 1107-1110.	4.6	34
99	Tumor Microenvironment-Responsive Cu <sub>2</sub> (OH)PO <sub>4</sub> Nanocrystals for Selective and Controllable Radiosentization via the X-ray-Triggered Fenton-like Reaction. Nano Letters, 2019, 19, 1749-1757.	4.5	142
100	Translocation, biotransformation-related degradation, and toxicity assessment of polyvinylpyrrolidone-modified 2H-phase nano-MoS <sub>2</sub> . Nanoscale, 2019, 11, 4767-4780.	2.8	47
101	A tumour-selective cascade activatable self-detained system for drug delivery and cancer imaging. Nature Communications, 2019, 10, 4861.	5.8	139
102	A photochromic upconversion nanoarchitecture: towards activatable bioimaging and dual NIR light-programmed singlet oxygen generation. Chemical Science, 2019, 10, 10231-10239.	3.7	45
103	Emerging Strategies of Nanomaterialâ€Mediated Tumor Radiosensitization. Advanced Materials, 2019, 31, e1802244.	11.1	244
104	Generalized Preparation of Two-Dimensional Quasi-nanosheets via Self-assembly of Nanoparticles. Journal of the American Chemical Society, 2019, 141, 1725-1734.	6.6	29
105	Tumor microenvironment-manipulated radiocatalytic sensitizer based on bismuth heteropolytungstate for radiotherapy enhancement. Biomaterials, 2019, 189, 11-22.	5.7	132
106	Boron and Nitrogen Co-Doping of Graphynes without Inducing Empty or Doubly Filled States in ï€-Conjugated Systems. Journal of Physical Chemistry C, 2019, 123, 625-630.	1.5	2
107	Engineering Multifunctional DNA Hybrid Nanospheres through Coordinationâ€Driven Selfâ€Assembly. Angewandte Chemie, 2019, 131, 1364-1368.	1.6	26
108	Engineering Multifunctional DNA Hybrid Nanospheres through Coordinationâ€Driven Selfâ€Assembly. Angewandte Chemie - International Edition, 2019, 58, 1350-1354.	7.2	149

#	Article	IF	CITATIONS
109	Graphdiyne Nanoparticles with High Free Radical Scavenging Activity for Radiation Protection. ACS Applied Materials & Interfaces, 2019, 11, 2579-2590.	4.0	115
110	Immobilized Ferrous Ion and Glucose Oxidase on Graphdiyne and Its Application on One-Step Glucose Detection. ACS Applied Materials & amp; Interfaces, 2019, 11, 2647-2654.	4.0	86
111	Turning On/Off the Anti-Tumor Effect of the Au Cluster via Atomically Controlling Its Molecular Size. ACS Nano, 2018, 12, 4378-4386.	7.3	34
112	Probing Adsorption Behaviors of BSA onto Chiral Surfaces of Nanoparticles. Small, 2018, 14, e1703982.	5.2	73
113	Graphdiyne Nanosheet-Based Drug Delivery Platform for Photothermal/Chemotherapy Combination Treatment of Cancer. ACS Applied Materials & Interfaces, 2018, 10, 8436-8442.	4.0	130
114	Acute Oral Administration of Singleâ€Walled Carbon Nanotubes Increases Intestinal Permeability and Inflammatory Responses: Association with the Changes in Gut Microbiota in Mice. Advanced Healthcare Materials, 2018, 7, e1701313.	3.9	40
115	A DNA nanorobot functions as a cancer therapeutic in response to a molecular trigger in vivo. Nature Biotechnology, 2018, 36, 258-264.	9.4	1,066
116	Intelligent MoS <sub>2</sub> Nanotheranostic for Targeted and Enzyme-/pH-/NIR-Responsive Drug Delivery To Overcome Cancer Chemotherapy Resistance Guided by PET Imaging. ACS Applied Materials & Interfaces, 2018, 10, 4271-4284.	4.0	137
117	Early-life exposure to three size-fractionated ultrafine and fine atmospheric particulates in Beijing exacerbates asthma development in mature mice. Particle and Fibre Toxicology, 2018, 15, 13.	2.8	53
118	Specific detection and effective inhibition of a single bacterial species in situ using peptide mineralized Au cluster probes. Science China Chemistry, 2018, 61, 627-634.	4.2	12
119	Nucleosome-inspired nanocarrier obtains encapsulation efficiency enhancement and side effects reduction in chemotherapy by using fullerenol assembled with doxorubicin. Biomaterials, 2018, 167, 205-215.	5.7	57
120	Quantification of Nanomaterial/Nanomedicine Trafficking in Vivo. Analytical Chemistry, 2018, 90, 589-614.	3.2	85
121	Solidifying framework nucleic acids. Science China Chemistry, 2018, 61, 1481-1482.	4.2	0
122	Precise nanomedicine for intelligent therapy of cancer. Science China Chemistry, 2018, 61, 1503-1552.	4.2	336
123	Ultrasensitive Detection of Serum MicroRNA Using Branched DNA-Based SERS Platform Combining Simultaneous Detection of α-Fetoprotein for Early Diagnosis of Liver Cancer. ACS Applied Materials & Interfaces, 2018, 10, 34869-34877.	4.0	60
124	Mechanisms of Antioxidant Activities of Fullerenols from First-Principles Calculation. Journal of Physical Chemistry A, 2018, 122, 8183-8190.	1.1	27
125	The Precise Diagnosis of Cancer Invasion/Metastasis <i>via</i> 2D Laser Ablation Mass Mapping of Metalloproteinase in Primary Cancer Tissue. ACS Nano, 2018, 12, 11139-11151.	7.3	29
126	Functionalized MoS <sub>2</sub> Nanovehicle with Nearâ€Infrared Laserâ€Mediated Nitric Oxide Release and Photothermal Activities for Advanced Bacteriaâ€Infected Wound Therapy. Small, 2018, 14, e1802290.	5.2	259

#	Article	IF	CITATIONS
127	Frontispiece: Simultaneous Quantification of Multiple Cancer Biomarkers in Blood Samples through DNA-Assisted Nanopore Sensing. Angewandte Chemie - International Edition, 2018, 57, .	7.2	1
128	Frontispiz: Simultaneous Quantification of Multiple Cancer Biomarkers in Blood Samples through DNA-Assisted Nanopore Sensing. Angewandte Chemie, 2018, 130, .	1.6	0
129	Xâ€Rayâ€Controlled Generation of Peroxynitrite Based on Nanosized LiLuF <sub>4</sub> :Ce <sup>3+</sup> Scintillators and their Applications for Radiosensitization. Advanced Materials, 2018, 30, e1804046.	11.1	138
130	Simultaneous Quantification of Multiple Cancer Biomarkers in Blood Samples through DNAâ€Assisted Nanopore Sensing. Angewandte Chemie, 2018, 130, 12058-12063.	1.6	13
131	Simultaneous Quantification of Multiple Cancer Biomarkers in Blood Samples through DNAâ€Assisted Nanopore Sensing. Angewandte Chemie - International Edition, 2018, 57, 11882-11887.	7.2	77
132	Frequency Shift Raman-Based Sensing of Serum MicroRNAs for Early Diagnosis and Discrimination of Primary Liver Cancers. Analytical Chemistry, 2018, 90, 10144-10151.	3.2	38
133	Harnessing Tumor Microenvironment for Nanoparticleâ€Mediated Radiotherapy. Advanced Therapeutics, 2018, 1, 1800050.	1.6	33
134	One Second Formation of Large Area Graphene on a Conical Tip Surface via Direct Transformation of Surface Carbide. Small, 2018, 14, e1801288.	5.2	3
135	Trophic Transfer and Transformation of CeO <sub>2</sub> Nanoparticles along a Terrestrial Food Chain: Influence of Exposure Routes. Environmental Science & Technology, 2018, 52, 7921-7927.	4.6	49
136	Gut Microbiota: Acute Oral Administration of Singleâ€Walled Carbon Nanotubes Increases Intestinal Permeability and Inflammatory Responses: Association with the Changes in Gut Microbiota in Mice (Adv. Healthcare Mater. 13/2018). Advanced Healthcare Materials, 2018, 7, 1870053.	3.9	0
137	Application of Multifunctional Nanomaterials in Radioprotection of Healthy Tissues. Advanced Healthcare Materials, 2018, 7, e1800421.	3.9	52
138	A Sizeâ€Reducible Nanodrug with an Aggregationâ€Enhanced Photodynamic Effect for Deep Chemoâ€Photodynamic Therapy. Angewandte Chemie, 2018, 130, 11554-11558.	1.6	29
139	A Sizeâ€Reducible Nanodrug with an Aggregationâ€Enhanced Photodynamic Effect for Deep Chemoâ€Photodynamic Therapy. Angewandte Chemie - International Edition, 2018, 57, 11384-11388.	7.2	196
140	Walking the line: The fate of nanomaterials at biological barriers. Biomaterials, 2018, 174, 41-53.	5.7	125
141	In Situ Monitoring the Aggregation Dynamics of Amyloid-β Protein Aβ42 in Physiological Media via a Raman-Based Frequency Shift Method. ACS Applied Bio Materials, 2018, 1, 814-824.	2.3	21
142	Reversal of pancreatic desmoplasia by re-educating stellate cells with a tumour microenvironment-activated nanosystem. Nature Communications, 2018, 9, 3390.	5.8	249
143	Cd@C82(OH)22 harnesses inflammatory regeneration for osteogenesis of mesenchymal stem cells through JNK/STAT3 signaling pathway. Journal of Materials Chemistry B, 2018, 6, 5802-5811.	2.9	12
144	mTOR Signaling in Parkinson's Disease. NeuroMolecular Medicine, 2017, 19, 1-10.	1.8	74

#	Article	IF	CITATIONS
145	A highly sensitive SERS-based platform for Zn( <scp>ii</scp> ) detection in cellular media. Chemical Communications, 2017, 53, 1797-1800.	2.2	23
146	Size-Dependent Ag <sub>2</sub> S Nanodots for Second Near-Infrared Fluorescence/Photoacoustics Imaging and Simultaneous Photothermal Therapy. ACS Nano, 2017, 11, 1848-1857.	7.3	351
147	Biodistribution, excretion, and toxicity of polyethyleneimine modified NaYF <sub>4</sub> :Yb,Er upconversion nanoparticles in mice via different administration routes. Nanoscale, 2017, 9, 4497-4507.	2.8	61
148	Protein-directed synthesis of Bi <sub>2</sub> S <sub>3</sub> nanoparticles as an efficient contrast agent for visualizing the gastrointestinal tract. RSC Advances, 2017, 7, 17505-17513.	1.7	15
149	Design of TPGS-functionalized Cu <sub>3</sub> BiS <sub>3</sub> nanocrystals with strong absorption in the second near-infrared window for radiation therapy enhancement. Nanoscale, 2017, 9, 8229-8239.	2.8	69
150	Chiral Surface of Nanoparticles Determines the Orientation of Adsorbed Transferrin and Its Interaction with Receptors. ACS Nano, 2017, 11, 4606-4616.	7.3	125
151	Polyoxometalate-Based Radiosensitization Platform for Treating Hypoxic Tumors by Attenuating Radioresistance and Enhancing Radiation Response. ACS Nano, 2017, 11, 7164-7176.	7.3	168
152	Ceria Nanoparticles as Enzyme Mimetics. Chinese Journal of Chemistry, 2017, 35, 791-800.	2.6	40
153	MoS <sub>2</sub> -Nanosheet-Assisted Coordination of Metal Ions with Porphyrin for Rapid Detection and Removal of Cadmium Ions in Aqueous Media. ACS Applied Materials & amp; Interfaces, 2017, 9, 21362-21370.	4.0	54
154	Photodynamic Therapy: Au Nanoclusters and Photosensitizer Dual Loaded Spatiotemporal Controllable Liposomal Nanocomposites Enhance Tumor Photodynamic Therapy Effect by Inhibiting Thioredoxin Reductase (Adv. Healthcare Mater. 7/2017). Advanced Healthcare Materials, 2017, 6, .	3.9	0
155	Therapeutic Nanoparticles Based on Curcumin and Bamboo Charcoal Nanoparticles for Chemo-Photothermal Synergistic Treatment of Cancer and Radioprotection of Normal Cells. ACS Applied Materials & Interfaces, 2017, 9, 14281-14291.	4.0	72
156	Fullerenol inhibits the cross-talk between bone marrow-derived mesenchymal stem cells and tumor cells by regulating MAPK signaling. Nanomedicine: Nanotechnology, Biology, and Medicine, 2017, 13, 1879-1890.	1.7	16
157	Diverse Applications of Nanomedicine. ACS Nano, 2017, 11, 2313-2381.	7.3	976
158	Au Nanoclusters and Photosensitizer Dual Loaded Spatiotemporal Controllable Liposomal Nanocomposites Enhance Tumor Photodynamic Therapy Effect by Inhibiting Thioredoxin Reductase. Advanced Healthcare Materials, 2017, 6, 1601453.	3.9	30
159	Bifunctional Tellurium Nanodots for Photo-Induced Synergistic Cancer Therapy. ACS Nano, 2017, 11, 10012-10024.	7.3	151
160	Synthesis of BSAâ€Coated BiOI@Bi <sub>2</sub> S <sub>3</sub> Semiconductor Heterojunction Nanoparticles and Their Applications for Radio/Photodynamic/Photothermal Synergistic Therapy of Tumor. Advanced Materials, 2017, 29, 1704136.	11.1	257
161	Elemental Bismuth–Graphene Heterostructures for Photocatalysis from Ultraviolet to Infrared Light. ACS Catalysis, 2017, 7, 7043-7050.	5.5	65
162	Photothermal Effect Enhanced Cascade-Targeting Strategy for Improved Pancreatic Cancer Therapy by Gold Nanoshell@Mesoporous Silica Nanorod. ACS Nano, 2017, 11, 8103-8113.	7.3	135

#	Article	IF	CITATIONS
163	Poly(Vinylpyrollidone)―and Selenocysteineâ€Modified Bi <sub>2</sub> Se <sub>3</sub> Nanoparticles Enhance Radiotherapy Efficacy in Tumors and Promote Radioprotection in Normal Tissues. Advanced Materials, 2017, 29, 1701268.	11.1	171
164	Metallofullerenol Inhibits Cellular Iron Uptake by Inducing Transferrin Tetramerization. Chemistry - an Asian Journal, 2017, 12, 2646-2651.	1.7	8
165	The effects of orally administered Ag, TiO 2 and SiO 2 nanoparticles on gut microbiota composition and colitis induction in mice. NanoImpact, 2017, 8, 80-88.	2.4	139
166	Ultrasmall Superparamagnetic Iron Oxide Nanoparticle for <i>T</i> <sub>2</sub> -Weighted Magnetic Resonance Imaging. ACS Applied Materials & Interfaces, 2017, 9, 28959-28966.	4.0	61
167	Design, Synthesis, and Surface Modification of Materials Based on Transitionâ€Metal Dichalcogenides for Biomedical Applications. Small Methods, 2017, 1, 1700220.	4.6	86
168	Strategies for improving drug delivery: nanocarriers and microenvironmental priming. Expert Opinion on Drug Delivery, 2017, 14, 865-877.	2.4	39
169	Study on orally delivered paclitaxel nanocrystals: modification, characterization and activity in the gastrointestinal tract. Royal Society Open Science, 2017, 4, 170753.	1.1	3
170	Comparison of cellular effects of starch-coated SPIONs and poly(lactic-co-glycolic acid) matrix nanoparticles on human monocytes. International Journal of Nanomedicine, 2016, Volume 11, 5221-5236.	3.3	23
171	A pyruvate decarboxylase-mediated therapeutic strategy for mimicking yeast metabolism in cancer cells. Pharmacological Research, 2016, 111, 413-421.	3.1	7
172	Mesoporous Bamboo Charcoal Nanoparticles as a New Nearâ€Infrared Responsive Drug Carrier for Imagingâ€Guided Chemotherapy/Photothermal Synergistic Therapy of Tumor. Advanced Healthcare Materials, 2016, 5, 1627-1637.	3.9	34
173	Single-pulse enhanced coherent diffraction imaging of bacteria with an X-ray free-electron laser. Scientific Reports, 2016, 6, 34008.	1.6	22
174	Multifunctional WS <sub>2</sub> @Poly(ethylene imine) Nanoplatforms for Imaging Guided Geneâ€Photothermal Synergistic Therapy of Cancer. Advanced Healthcare Materials, 2016, 5, 2776-2787.	3.9	86
175	Bifunctional Platinated Nanoparticles for Photoinduced Tumor Ablation. Advanced Materials, 2016, 28, 10155-10164.	11.1	170
176	Gdâ€Hybridized Plasmonic Auâ€Nanocomposites Enhanced Tumorâ€Interior Drug Permeability in Multimodal Imagingâ€Guided Therapy. Advanced Materials, 2016, 28, 8950-8958.	11.1	138
177	Cold Nanomaterials in Consumer Cosmetics Nanoproducts: Analyses, Characterization, and Dermal Safety Assessment. Small, 2016, 12, 5488-5496.	5.2	55
178	Photothermal Therapy: Multifunctional WS2 @Polyetherimide Nanoplatforms for Imaging Guided Gene-Photothermal Synergistic Therapy of Cancer (Adv. Healthcare Mater. 21/2016). Advanced Healthcare Materials, 2016, 5, 2834-2834.	3.9	1
179	Functionalized Nano-MoS <sub>2</sub> with Peroxidase Catalytic and Near-Infrared Photothermal Activities for Safe and Synergetic Wound Antibacterial Applications. ACS Nano, 2016, 10, 11000-11011.	7.3	812
180	Gadolinium polytungstate nanoclusters: a new theranostic with ultrasmall size and versatile properties for dual-modal MR/CT imaging and photothermal therapy/radiotherapy of cancer. NPG Asia Materials, 2016, 8, e273-e273.	3.8	75

#	Article	IF	CITATIONS
181	Proteinâ€Nanoreactorâ€Assisted Synthesis of Semiconductor Nanocrystals for Efficient Cancer Theranostics. Advanced Materials, 2016, 28, 5923-5930.	11.1	175
182	High-Throughput Screening of Substrate Specificity for Protein Tyrosine Phosphatases (PTPs) on Phosphopeptide Microarrays. Methods in Molecular Biology, 2016, 1368, 181-196.	0.4	14
183	SERS-based sensing technique for trace melamine detection – A new method exploring. Talanta, 2016, 153, 186-190.	2.9	19
184	Fluorescent supramolecular micelles for imaging-guided cancer therapy. Nanoscale, 2016, 8, 5302-5312.	2.8	32
185	Investigating the stability of gold nanorods modified with thiol molecules for biosensing. RSC Advances, 2016, 6, 174-178.	1.7	3
186	Ultrasensitive, Multiplex Raman Frequency Shift Immunoassay of Liver Cancer Biomarkers in Physiological Media. ACS Nano, 2016, 10, 871-879.	7.3	91
187	Aspect ratios of gold nanoshell capsules mediated melanoma ablation by synergistic photothermal therapy and chemotherapy. Nanomedicine: Nanotechnology, Biology, and Medicine, 2016, 12, 439-448.	1.7	41
188	Polyhydroxylated fullerenols regulate macrophage for cancer adoptive immunotherapy and greatly inhibit the tumor metastasis. Nanomedicine: Nanotechnology, Biology, and Medicine, 2016, 12, 945-954.	1.7	46
189	Theoretical studies on the complexation of Eu(III) and Am(III) with HDEHP: structure, bonding nature and stability. Science China Chemistry, 2016, 59, 324-331.	4.2	29
190	One-pot synthesis of PEGylated plasmonic MoO3–x hollow nanospheres for photoacoustic imaging guided chemo-photothermal combinational therapy of cancer. Biomaterials, 2016, 76, 11-24.	5.7	171
191	A thiol fluorescent probe reveals the intricate modulation of cysteine's reactivity by Cu(II). Talanta, 2016, 146, 477-482.	2.9	21
192	Smart Albuminâ€Biomineralized Nanocomposites for Multimodal Imaging and Photothermal Tumor Ablation. Advanced Materials, 2015, 27, 3874-3882.	11.1	278
193	Tetranuclear Uranyl Polyrotaxanes: Preferred Selectivity toward Uranyl Tetramer for Stabilizing a Flexible Polyrotaxane Chain Exhibiting Weakened Supramolecular Inclusion. Chemistry - A European Journal, 2015, 21, 10226-10235.	1.7	27
194	Recent Advances in Upconversion Nanoparticlesâ€Based Multifunctional Nanocomposites for Combined Cancer Therapy. Advanced Materials, 2015, 27, 7692-7712.	11.1	243
195	Coculture with Lowâ€Dose SWCNT Attenuates Bacterial Invasion and Inflammation in Human Enterocyteâ€like Cacoâ€⊋ Cells. Small, 2015, 11, 4366-4378.	5.2	18
196	Polydopamine as a Biocompatible Multifunctional Nanocarrier for Combined Radioisotope Therapy and Chemotherapy of Cancer. Advanced Functional Materials, 2015, 25, 7327-7336.	7.8	225
197	Phytotoxicity, Translocation, and Biotransformation of NaYF <sub>4</sub> Upconversion Nanoparticles in a Soybean Plant. Small, 2015, 11, 4774-4784.	5.2	49
198	Smart MoS <sub>2</sub> /Fe <sub>3</sub> O <sub>4</sub> Nanotheranostic for Magnetically Targeted Photothermal Therapy Guided by Magnetic Resonance/Photoacoustic Imaging. Theranostics, 2015, 5, 931-945.	4.6	234

#	Article	IF	CITATIONS
199	Use of Synchrotron Radiation-Analytical Techniques To Reveal Chemical Origin of Silver-Nanoparticle Cytotoxicity. ACS Nano, 2015, 9, 6532-6547.	7.3	246
200	Transformation of ceria nanoparticles in cucumber plants is influenced by phosphate. Environmental Pollution, 2015, 198, 8-14.	3.7	84
201	Evaluation of the influence of fullerenol on aging and stress resistance using Caenorhabditis elegans. Biomaterials, 2015, 42, 78-86.	5.7	43
202	Near-infrared light remote-controlled intracellular anti-cancer drug delivery using thermo/pH sensitive nanovehicle. Acta Biomaterialia, 2015, 17, 201-209.	4.1	145
203	Efficient removal of uranium from aqueous solution by zero-valent iron nanoparticle and its graphene composite. Journal of Hazardous Materials, 2015, 290, 26-33.	6.5	231
204	Halogen Bonded Three-Dimensional Uranyl–Organic Compounds with Unprecedented Halogen–Halogen Interactions and Structure Diversity upon Variation of Halogen Substitution. Crystal Growth and Design, 2015, 15, 1395-1406.	1.4	36
205	Facile Approach To Observe and Quantify the α <sub>Ilb</sub> β <sub>3</sub> Integrin on a Single-Cell. Analytical Chemistry, 2015, 87, 2546-2549.	3.2	53
206	Bismuth Sulfide Nanorods as a Precision Nanomedicine for <i>in Vivo</i> Multimodal Imaging-Guided Photothermal Therapy of Tumor. ACS Nano, 2015, 9, 696-707.	7.3	503
207	Gd-metallofullerenol nanomaterial as non-toxic breast cancer stem cell-specific inhibitor. Nature Communications, 2015, 6, 5988.	5.8	164
208	Nanosurface chemistry and dose govern the bioaccumulation and toxicity of carbon nanotubes, metal nanomaterials and quantum dots in vivo. Science Bulletin, 2015, 60, 3-20.	4.3	96
209	Label-Free Au Cluster Used for in Vivo 2D and 3D Computed Tomography of Murine Kidneys. Analytical Chemistry, 2015, 87, 343-345.	3.2	48
210	Gd–Metallofullerenol Nanomaterial Suppresses Pancreatic Cancer Metastasis by Inhibiting the Interaction of Histone Deacetylase 1 and Metastasis-Associated Protein 1. ACS Nano, 2015, 9, 6826-6836.	7.3	64
211	Ultrasmall [ <sup>64</sup> Cu]Cu Nanoclusters for Targeting Orthotopic Lung Tumors Using Accurate Positron Emission Tomography Imaging. ACS Nano, 2015, 9, 4976-4986.	7.3	108
212	Enhanced Multifunctional Properties of Graphene Nanocomposites with Nacre‣ike Structures. Advanced Engineering Materials, 2015, 17, 523-531.	1.6	15
213	Probing the interaction at nano-bio interface using synchrotron radiation-based analytical techniques. Science China Chemistry, 2015, 58, 768-779.	4.2	28
214	Controllable Generation of Nitric Oxide by Nearâ€Infraredâ€Sensitized Upconversion Nanoparticles for Tumor Therapy. Advanced Functional Materials, 2015, 25, 3049-3056.	7.8	194
215	Two novel uranyl complexes of a semi-rigid aromatic tetracarboxylic acid supported by an organic base as an auxiliary ligand or a templating agent: an experimental and theoretical exploration. CrystEngComm, 2015, 17, 3031-3040.	1.3	16
216	Synchrotron radiation techniques for nanotoxicology. Nanomedicine: Nanotechnology, Biology, and Medicine, 2015, 11, 1531-1549.	1.7	29

#	Article	IF	CITATIONS
217	Peptide-Conjugated Gold Nanoprobe: Intrinsic Nanozyme-Linked Immunsorbant Assay of Integrin Expression Level on Cell Membrane. ACS Nano, 2015, 9, 10979-10990.	7.3	99
218	Tungsten Sulfide Quantum Dots as Multifunctional Nanotheranostics for <i>In Vivo</i> Dual-Modal Image-Guided Photothermal/Radiotherapy Synergistic Therapy. ACS Nano, 2015, 9, 12451-12463.	7.3	388
219	The isotopic effects of <sup>13</sup> C-labeled large carbon cage (C <sub>70</sub> ) fullerenes and their formation process. RSC Advances, 2015, 5, 76949-76956.	1.7	14
220	A Quasi-relativistic Density Functional Theory Study of the Actinyl(VI, V) (An = U, Np, Pu) Complexes with a Six-Membered Macrocycle Containing Pyrrole, Pyridine, and Furan Subunits. Journal of Physical Chemistry A, 2015, 119, 9178-9188.	1.1	35
221	Protein Corona Influences Cellular Uptake of Gold Nanoparticles by Phagocytic and Nonphagocytic Cells in a Size-Dependent Manner. ACS Applied Materials & Interfaces, 2015, 7, 20568-20575.	4.0	243
222	Quantifying the distribution of ceria nanoparticles in cucumber roots: the influence of labeling. RSC Advances, 2015, 5, 4554-4560.	1.7	18
223	Where Does the Transformation of Precipitated Ceria Nanoparticles in Hydroponic Plants Take Place?. Environmental Science & Technology, 2015, 49, 10667-10674.	4.6	82
224	Smart Cu1.75S nanocapsules with high and stable photothermal efficiency for NIR photo-triggered drug release. Nano Research, 2015, 8, 4038-4047.	5.8	52
225	Origin of the different phytotoxicity and biotransformation of cerium and lanthanum oxide nanoparticles in cucumber. Nanotoxicology, 2015, 9, 262-270.	1.6	123
226	TPGS-stabilized NaYbF4:Er upconversion nanoparticles for dual-modal fluorescent/CT imaging and anticancer drug delivery to overcome multi-drug resistance. Biomaterials, 2015, 40, 107-116.	5.7	172
227	Species-specific toxicity of ceria nanoparticles to <i>Lactuca</i> plants. Nanotoxicology, 2015, 9, 1-8.	1.6	106
228	Luminescent Nanoparticles: Elimination of Photon Quenching by a Transition Layer to Fabricate a Quenchingâ€Shield Sandwich Structure for 800 nm Excited Upconversion Luminescence of Nd <sup>3+</sup> â€Sensitized Nanoparticles (Adv. Mater. 18/2014). Advanced Materials, 2014, 26, 2766-2766.	11.1	2
229	Polyhydroxylated Metallofullerenols Stimulate ILâ€1β Secretion of Macrophage through TLRs/MyD88/NFâ€₽B Pathway and NLRP <sub>3</sub> Inflammasome Activation. Small, 2014, 10, 2362-2372.	5.2	96
230	Growth of Uranyl Hydroxide Nanowires and Nanotubes by the Electrodeposition Method and Their Transformation to One-Dimensional U3O8Nanostructures. European Journal of Inorganic Chemistry, 2014, 2014, 1158-1164.	1.0	14
231	Novel Insights into Combating Cancer Chemotherapy Resistance Using a Plasmonic Nanocarrier: Enhancing Drug Sensitiveness and Accumulation Simultaneously with Localized Mild Photothermal Stimulus of Femtosecond Pulsed Laser. Advanced Functional Materials, 2014, 24, 4229-4239.	7.8	130
232	A density functional theory study of complex species and reactions of Am(III)/Eu(III) with nitrate anions. Molecular Simulation, 2014, 40, 379-386.	0.9	17
233	Assembling single gold nanorods into large-scale highly aligned nanoarrays via vacuum-enhanced capillarity. Nanoscale Research Letters, 2014, 9, 556.	3.1	2
234	Extraction complexes of Pu(IV) with carbamoylmethylphosphine oxide ligands: AÂrelativistic density functional study. Radiochimica Acta, 2014, 102, 77-86.	0.5	9

#	Article	IF	CITATIONS
235	Synthesis of ordered mesoporous U <sub>3</sub> O <sub>8</sub> by a nanocasting route. Radiochimica Acta, 2014, 102, 813-816.	0.5	3
236	Selective separation of Am(III) from Eu(III) by 2,9-Bis(dialkyl-1,2,4-triazin-3-yl)-1,10-phenanthrolines: a relativistic quantum chemistry study. Radiochimica Acta, 2014, 102, 875-886.	0.5	18
237	Solvent extraction of uranium(VI) by aÂdipicolinamide using aÂroom-temperature ionic liquid. Radiochimica Acta, 2014, 102, 87-92.	0.5	21
238	Enhanced endosomal/lysosomal escape by distearoyl phosphoethanolamine-polycarboxybetaine lipid for systemic delivery of siRNA. Journal of Controlled Release, 2014, 176, 104-114.	4.8	102
239	Regulation on mechanical properties of collagen: Enhanced bioactivities of metallofullerol. Nanomedicine: Nanotechnology, Biology, and Medicine, 2014, 10, 783-793.	1.7	12
240	A facile additive-free method for tunable fabrication of UO2 and U3O8 nanoparticles in aqueous solution. CrystEngComm, 2014, 16, 2645.	1.3	38
241	The nano-plasma interface: Implications of the protein corona. Colloids and Surfaces B: Biointerfaces, 2014, 124, 17-24.	2.5	155
242	A magnetic graphene hybrid functionalized with beta-cyclodextrins for fast and efficient removal of organic dyes. Journal of Materials Chemistry A, 2014, 2, 12296.	5.2	113
243	Shrinkage of pegylated and non-pegylated liposomes in serum. Colloids and Surfaces B: Biointerfaces, 2014, 114, 294-300.	2.5	96
244	Quantification of carbon nanomaterials in vivo: direct stable isotope labeling on the skeleton of fullerene C <sub>60</sub> . Environmental Science: Nano, 2014, 1, 64-70.	2.2	26
245	Toxicity of inorganic nanomaterials in biomedical imaging. Biotechnology Advances, 2014, 32, 727-743.	6.0	94
246	Solvent extraction of U(VI) by trioctylphosphine oxide using a room-temperature ionic liquid. Science China Chemistry, 2014, 57, 1432-1438.	4.2	48
247	Integration of Nanoassembly Functions for an Effective Delivery Cascade for Cancer Drugs. Advanced Materials, 2014, 26, 7615-7621.	11.1	317
248	Localized Electric Field of Plasmonic Nanoplatform Enhanced Photodynamic Tumor Therapy. ACS Nano, 2014, 8, 11529-11542.	7.3	220
249	Interactions between Th( <scp>iv</scp> ) and graphene oxide: experimental and density functional theoretical investigations. RSC Advances, 2014, 4, 3340-3347.	1.7	56
250	On-demand generation of singlet oxygen from a smart graphene complex for the photodynamic treatment of cancer cells. Biomaterials Science, 2014, 2, 1412-1418.	2.6	26
251	Regioselective alkyl transfer from phosphonium ylides to functionalized polyfluoroarenes. Chemical Science, 2014, 5, 1934-1939.	3.7	19
252	A precision structural model for fullerenols. Chemical Science, 2014, 5, 2940-2948.	3.7	43

#	Article	IF	CITATIONS
253	Design criteria for tetradentate phenanthroline-derived heterocyclic ligands to separate Am(III) from Eu(III). Science China Chemistry, 2014, 57, 1439-1448.	4.2	13
254	Mesoporous NaYbF4@NaGdF4 core-shell up-conversion nanoparticles for targeted drug delivery and multimodal imaging. Biomaterials, 2014, 35, 7666-7678.	5.7	94
255	WS <sub>2</sub> nanosheet as a new photosensitizer carrier for combined photodynamic and photothermal therapy of cancer cells. Nanoscale, 2014, 6, 10394-10403.	2.8	301
256	Near Infrared Laser-Induced Targeted Cancer Therapy Using Thermoresponsive Polymer Encapsulated Gold Nanorods. Journal of the American Chemical Society, 2014, 136, 7317-7326.	6.6	569
257	Visual detection of Cu( <scp>ii</scp> ) ions based on a simple pyrene derivative using click chemistry. Analytical Methods, 2014, 6, 4977-4981.	1.3	11
258	Metallofullerenols: Polyhydroxylated Metallofullerenols Stimulate IL-1β Secretion of Macrophage through TLRs/MyD88/NF-κB Pathway and NLRP3Inflammasome Activation (Small 12/2014). Small, 2014, 10, 2310-2310.	5.2	2
259	High-Throughput Synthesis of Single-Layer MoS <sub>2</sub> Nanosheets as a Near-Infrared Photothermal-Triggered Drug Delivery for Effective Cancer Therapy. ACS Nano, 2014, 8, 6922-6933.	7.3	813
260	Rotation Motion of Designed Nano-Turbine. Scientific Reports, 2014, 4, 5846.	1.6	27
261	Recent Advances in Design and Fabrication of Upconversion Nanoparticles and Their Safe Theranostic Applications. Advanced Materials, 2013, 25, 3758-3779.	11.1	437
262	Surface chemistry of gold nanorods: origin of cell membrane damage and cytotoxicity. Nanoscale, 2013, 5, 8384.	2.8	141
263	Advanced nuclear analytical and related techniques for the growing challenges in nanotoxicology. Chemical Society Reviews, 2013, 42, 8266.	18.7	104
264	Broad‣pectrum Antibacterial Activity of Carbon Nanotubes to Human Gut Bacteria. Small, 2013, 9, 2735-2746.	5.2	236
265	First-principles DFT+U modeling of defect behaviors in anti-ferromagnetic uranium mononitride. Journal of Applied Physics, 2013, 114, .	1.1	21
266	Biological characterizations of [Gd@C82(OH)22] <i>n</i> nanoparticles as fullerene derivatives for cancer therapy. Integrative Biology (United Kingdom), 2013, 5, 43-47.	0.6	76
267	First principles modeling of zirconium solution in bulk UO2. Journal of Applied Physics, 2013, 113, .	1.1	22
268	Two new uranyl fluoride complexes with UVlî€O–alkali (Na, Cs) interactions: Experimental and theoretical studies. CrystEngComm, 2013, 15, 8041.	1.3	8
269	Physicochemical Properties Determine Nanomaterial Cellular Uptake, Transport, and Fate. Accounts of Chemical Research, 2013, 46, 622-631.	7.6	627
270	Revealing the Binding Structure of the Protein Corona on Gold Nanorods Using Synchrotron Radiation-Based Techniques: Understanding the Reduced Damage in Cell Membranes. Journal of the American Chemical Society, 2013, 135, 17359-17368.	6.6	239

#	Article	IF	CITATIONS
271	Metabolism of Nanomaterials <i>in Vivo</i> : Blood Circulation and Organ Clearance. Accounts of Chemical Research, 2013, 46, 761-769.	7.6	424
272	Understanding the Toxicity of Carbon Nanotubes. Accounts of Chemical Research, 2013, 46, 702-713.	7.6	623
273	Interfacing Engineered Nanoparticles with Biological Systems: Anticipating Adverse Nano–Bio Interactions. Small, 2013, 9, 1573-1584.	5.2	176
274	Upconversion: Redâ€Emitting Upconverting Nanoparticles for Photodynamic Therapy in Cancer Cells Under Nearâ€Infrared Excitation (Small 11/2013). Small, 2013, 9, 1928-1928.	5.2	8
275	The contributions of metal impurities and tube structure to the toxicity of carbon nanotube materials. NPG Asia Materials, 2012, 4, e32-e32.	3.8	112
276	Molecular mechanism of pancreatic tumor metastasis inhibition by Gd@C <sub>82</sub> (OH) <sub>22</sub> and its implication for de novo design of nanomedicine. Proceedings of the National Academy of Sciences of the United States of America, 2012, 109, 15431-15436.	3.3	200
277	Nuclear and radiochemistry in China: present status and future perspectives. Radiochimica Acta, 2012, 100, 529-539.	0.5	9
278	Lanthanide-doped GdVO4 upconversion nanophosphors with tunable emissions and their applications for biomedical imaging. Journal of Materials Chemistry, 2012, 22, 6974.	6.7	124
279	Controllable synthesis of Gd2O(CO3)2·H2O@silica–FITC nanoparticles with size-dependent optical and magnetic resonance imaging properties. New Journal of Chemistry, 2012, 36, 2599.	1.4	15
280	TWEEN coated NaYF4:Yb,Er/NaYF4 core/shell upconversion nanoparticles for bioimaging and drug delivery. RSC Advances, 2012, 2, 7037.	1.7	98
281	Bifunctional peptides that precisely biomineralize Au clusters and specifically stain cell nuclei. Chemical Communications, 2012, 48, 871-873.	2.2	136
282	Microstructure evolution of diazonium functionalized graphene: A potential approach to change graphene electronic structure. Journal of Materials Chemistry, 2012, 22, 2063-2068.	6.7	38
283	Mesoporous silica SBA-15 functionalized with phosphonate and amino groups for uranium uptake. Science China Chemistry, 2012, 55, 1705-1711.	4.2	73
284	Graphene: Unraveling Stress-Induced Toxicity Properties of Graphene Oxide and the Underlying Mechanism (Adv. Mater. 39/2012). Advanced Materials, 2012, 24, 5390-5390.	11.1	2
285	Biotransformation of Ceria Nanoparticles in Cucumber Plants. ACS Nano, 2012, 6, 9943-9950.	7.3	319
286	Comparative toxicity of nanoparticulate/bulk Yb <sub>2</sub> O <sub>3</sub> and YbCl <sub>3</sub> to cucumber ( <i>Cucumis sativus</i> ). Environmental Science & Technology, 2012, 46, 1834-1841.	4.6	153
287	Size-tunable synthesis of lanthanide-doped Gd <sub>2</sub> O <sub>3</sub> nanoparticles and their applications for optical and magnetic resonance imaging. Journal of Materials Chemistry, 2012, 22, 966-974.	6.7	165
288	A novel mesoporous material for uranium extraction, dihydroimidazole functionalized SBA-15. Journal of Materials Chemistry, 2012, 22, 17019.	6.7	128

#	Article	IF	CITATIONS
289	Cold Nanorods: Watching Single Gold Nanorods Grow (Small 9/2012). Small, 2012, 8, 1290-1290.	5.2	0
290	Surface-Engineered Gold Nanorods: Promising DNA Vaccine Adjuvant for HIV-1 Treatment. Nano Letters, 2012, 12, 2003-2012.	4.5	282
291	A high efficient sorption of U(VI) from aqueous solution using amino-functionalized SBA-15. Journal of Radioanalytical and Nuclear Chemistry, 2012, 292, 803-810.	0.7	92
292	Gadolinium metallofullerenol nanoparticles inhibit cancer metastasis through matrix metalloproteinase inhibition: imprisoning instead of poisoning cancer cells. Nanomedicine: Nanotechnology, Biology, and Medicine, 2012, 8, 136-146.	1.7	101
293	Binding of blood proteins to carbon nanotubes reduces cytotoxicity. Proceedings of the National Academy of Sciences of the United States of America, 2011, 108, 16968-16973.	3.3	839
294	Quantification of proteins using lanthanide labeling and HPLC/ICP-MS detection. Journal of Analytical Atomic Spectrometry, 2011, 26, 1233.	1.6	19
295	Quantifying the biodistribution of nanoparticles. Nature Nanotechnology, 2011, 6, 755-755.	15.6	18
296	Controlling Assembly of Paired Gold Clusters within Apoferritin Nanoreactor for in Vivo Kidney Targeting and Biomedical Imaging. Journal of the American Chemical Society, 2011, 133, 8617-8624.	6.6	258
297	Selective Targeting of Gold Nanorods at the Mitochondria of Cancer Cells: Implications for Cancer Therapy. Nano Letters, 2011, 11, 772-780.	4.5	475
298	Separation of Hydrogen and Nitrogen Gases with Porous Graphene Membrane. Journal of Physical Chemistry C, 2011, 115, 23261-23266.	1.5	335
299	Full Assessment of Fate and Physiological Behavior of Quantum Dots Utilizing <i>Caenorhabditis elegans</i> as a Model Organism. Nano Letters, 2011, 11, 3174-3183.	4.5	212
300	Serial Silver Clusters Biomineralized by One Peptide. ACS Nano, 2011, 5, 8684-8689.	7.3	130
301	Uptake and distribution of ceria nanoparticles in cucumber plants. Metallomics, 2011, 3, 816.	1.0	226
302	Chirality of Glutathione Surface Coating Affects the Cytotoxicity of Quantum Dots. Angewandte Chemie - International Edition, 2011, 50, 5860-5864.	7.2	210
303	Direct evidence for catalase and peroxidase activities of ferritin–platinum nanoparticles. Biomaterials, 2011, 32, 1611-1618.	5.7	397
304	Phytotoxicity and biotransformation of La <sub>2</sub> O <sub>3</sub> nanoparticles in a terrestrial plant cucumber ( <i>Cucumis sativus</i> ). Nanotoxicology, 2011, 5, 743-753.	1.6	151
305	Surface chemistry and aspect ratio mediated cellular uptake of Au nanorods. Biomaterials, 2010, 31, 7606-7619.	5.7	613
306	Toxicity of zinc oxide nanoparticles to zebrafish embryo: a physicochemical study of toxicity mechanism. Journal of Nanoparticle Research, 2010, 12, 1645-1654.	0.8	348

#	Article	IF	CITATIONS
307	Lung deposition and extrapulmonary translocation of nano-ceria after intratracheal instillation. Nanotechnology, 2010, 21, 285103.	1.3	137
308	Effects of rare earth oxide nanoparticles on root elongation of plants. Chemosphere, 2010, 78, 273-279.	4.2	377
309	Chemistry of carbon nanotubes in biomedical applications. Journal of Materials Chemistry, 2010, 20, 1036-1052.	6.7	235
310	[Gd@C <sub>82</sub> (OH) <sub>22</sub> ] <sub><i>n</i></sub> Nanoparticles Induce Dendritic Cell Maturation and Activate Th1 Immune Responses. ACS Nano, 2010, 4, 1178-1186.	7.3	131
311	Potent Angiogenesis Inhibition by the Particulate Form of Fullerene Derivatives. ACS Nano, 2010, 4, 2773-2783.	7.3	148
312	Ecotoxicological assessment of lanthanum with Caenorhabditis elegans in liquid medium. Metallomics, 2010, 2, 806.	1.0	42
313	Metallofullerene nanoparticles circumvent tumor resistance to cisplatin by reactivating endocytosis. Proceedings of the National Academy of Sciences of the United States of America, 2010, 107, 7449-7454.	3.3	233
314	Quantitative imaging of element spatial distribution in the brain section of a mouse model of Alzheimer's disease using synchrotron radiation X-ray fluorescence analysis. Journal of Analytical Atomic Spectrometry, 2010, 25, 328-333.	1.6	54
315	Particokinetics and Extrapulmonary Translocation of Intratracheally Instilled Ferric Oxide Nanoparticles in Rats and the Potential Health Risk Assessment. Toxicological Sciences, 2009, 107, 342-351.	1.4	188
316	The effect of Gd@C82(OH)22 nanoparticles on the release of Th1/Th2 cytokines and induction of TNF-α mediated cellular immunity. Biomaterials, 2009, 30, 3934-3945.	5.7	177
317	Neurotoxicity of low-dose repeatedly intranasal instillation of nano- and submicron-sized ferric oxide particles in mice. Journal of Nanoparticle Research, 2009, 11, 41-53.	0.8	101
318	Applications of radiotracer techniques for the pharmacology and toxicology studies of nanomaterials. Science Bulletin, 2009, 54, 173-182.	4.3	17
319	The scavenging of reactive oxygen species and the potential for cell protection by functionalized fullerene materials. Biomaterials, 2009, 30, 611-621.	5.7	388
320	Acute toxicological impact of nano- and submicro-scaled zinc oxide powder on healthy adult mice. Journal of Nanoparticle Research, 2008, 10, 263-276.	0.8	338
321	The Growth of Complex Nanostructures: Synergism of Dipolar Force and Stackingâ€Đefects in Anisotropic Selfâ€Assembly. Advanced Materials, 2008, 20, 1794-1798.	11.1	8
322	Bio-distribution and metabolic paths of silica coated CdSeS quantum dots. Toxicology and Applied Pharmacology, 2008, 230, 364-371.	1.3	145
323	Potential neurological lesion after nasal instillation of TiO2 nanoparticles in the anatase and rutile crystal phases. Toxicology Letters, 2008, 183, 72-80.	0.4	310
324	Analysis of mercury-containing protein fractions in brain cytosol of the maternal and infant rats after exposure to a low-dose of methylmercury by SEC coupled to isotope dilution ICP-MS. Journal of Analytical Atomic Spectrometry, 2008, 23, 1112.	1.6	23

#	Article	IF	CITATIONS
325	Mapping technique for biodistribution of elements in a model organism, Caenorhabditis elegans, after exposure to copper nanoparticles with microbeam synchrotron radiation X-ray fluorescence. Journal of Analytical Atomic Spectrometry, 2008, 23, 1121.	1.6	75
326	The Strong MRI Relaxivity of Paramagnetic Nanoparticles. Journal of Physical Chemistry B, 2008, 112, 6288-6291.	1.2	51
327	Inhibition of Tumor Growth by Endohedral Metallofullerenol Nanoparticles Optimized as Reactive Oxygen Species Scavenger. Molecular Pharmacology, 2008, 74, 1132-1140.	1.0	117
328	Metallomics, elementomics, and analytical techniques. Pure and Applied Chemistry, 2008, 80, 2577-2594.	0.9	33
329	Rapid translocation and pharmacokinetics of hydroxylated single-walled carbon nanotubes in mice. Nanotoxicology, 2008, 2, 28-32.	1.6	41
330	Acute toxicity and biodistribution of different sized titanium dioxide particles in mice after oral administration. Toxicology Letters, 2007, 168, 176-185.	0.4	973
331	Simultaneous speciation of selenium and mercury in human urine samples from long-term mercury-exposed populations with supplementation of selenium-enriched yeast by HPLC-ICP-MS. Journal of Analytical Atomic Spectrometry, 2007, 22, 925.	1.6	50
332	Ytterbium and trace element distribution in brain and organic tissues of offspring rats after prenatal and postnatal exposure to ytterbium. Biological Trace Element Research, 2007, 117, 89-104.	1.9	25
333	5p Electronic properties of Gd in Gd@C82(OH)x studied by synchrotron radiation XPS. Journal of Radioanalytical and Nuclear Chemistry, 2007, 272, 307-310.	0.7	9
334	Uptake and elimination of lanthanum by excised roots of Triticum aestivum L Journal of Radioanalytical and Nuclear Chemistry, 2007, 272, 523-525.	0.7	2
335	Study of multihydroxylated processes of Gd@C82 by ICP-MASS. Journal of Radioanalytical and Nuclear Chemistry, 2007, 272, 537-540.	0.7	9
336	Ultrahigh reactivity and grave nanotoxicity of copper nanoparticles. Journal of Radioanalytical and Nuclear Chemistry, 2007, 272, 595-598.	0.7	30
337	Identification of target organs of copper nanoparticles with ICP-MS technique. Journal of Radioanalytical and Nuclear Chemistry, 2007, 272, 599-603.	0.7	45
338	Neutron-irradiation catalyzed synthesis of novel carbon nanomaterials. Journal of Radioanalytical and Nuclear Chemistry, 2007, 272, 611-614.	0.7	3
339	Elimination efficiency of different reagents for the memory effect of mercury using ICP-MS. Journal of Analytical Atomic Spectrometry, 2006, 21, 94-96.	1.6	322
340	Study of rare earth encapsulated carbon nanomolecules for biomedical uses. Journal of Alloys and Compounds, 2006, 408-412, 400-404.	2.8	28
341	In situ observation of C60(C(COOH)2)2 interacting with living cells using fluorescence microscopy. Science Bulletin, 2006, 51, 1060-1064.	1.7	18
342	XAFS study on interactions of metallothionein, mercuric chloride and/or sodium selenite. Diqiu Huaxue, 2006, 25, 124-124.	0.5	0

#	Article	IF	CITATIONS
343	Antioxidative function and biodistribution of [Gd@C82(OH)22]n nanoparticles in tumor-bearing mice. Biochemical Pharmacology, 2006, 71, 872-881.	2.0	152
344	Cytotoxicity of Carbon Nanomaterials:Â Single-Wall Nanotube, Multi-Wall Nanotube, and Fullerene. Environmental Science & Technology, 2005, 39, 1378-1383.	4.6	1,307
345	Multihydroxylated [Gd@C82(OH)22]nNanoparticles:Â Antineoplastic Activity of High Efficiency and Low Toxicity. Nano Letters, 2005, 5, 2050-2057.	4.5	281
346	Experiment on the Synthesis of Element 113 in the Reaction209Bi(70Zn,n)278113. Journal of the Physical Society of Japan, 2004, 73, 2593-2596.	0.7	479
347	Synthesis of new carbon nanomolecule: C141. Science Bulletin, 2004, 49, 793-796.	1.7	5
348	Highly Selective and Simple Synthesis of C2mâ^'Xâ^'C2nFullerene Dimers. Journal of the American Chemical Society, 2004, 126, 11134-11135.	6.6	38
349	Biodistribution of Carbon Single-Wall Carbon Nanotubes in Mice. Journal of Nanoscience and Nanotechnology, 2004, 4, 1019-1024.	0.9	355
350	Influences of Structural Properties on Stability of Fullerenols. Journal of Physical Chemistry B, 2004, 108, 11473-11479.	1.2	139
351	Spatially Selective Monitoring of Subcellular Enzyme Dynamics in Response to Mitochondriaâ€∓argeted Photodynamic Therapy. Angewandte Chemie, 0, , .	1.6	2
352	Mild Acidosisâ€Directed Signal Amplification in Tumor Microenvironment via Spatioselective Recruitment of DNA Amplifiers. Angewandte Chemie, 0, , .	1.6	0